IFSCC 2025 full paper (IFSCC2025-656)

"Flash Nano-Encapsulation of Probiotics for Gut-Skin Regulation: Functionalized Strains with High Endurance and Strong Mucin Adhesion"

Yongjie Lu [1], Bingqing Deng [1], Wenyun Zhang [1], Shaojie Gu [1], Weifan Niu [2], Zehao Qu [2], Tomoko Oto [3], Xiaozhi Wang [1], Jing Sun [1], Dongying Zhang [1], Yanbing Huang [4], Yu Lin [4], Shaochun Cai [5], Yan Huang [2,*] and Dongcui Li [1,*]

[1] Research and Development, Hua An Tang Biotech Group Co., Ltd., Guangzhou, China;
[2] Key Laboratory for Analytical Science of Food Safety and Biology, Ministry of Education; College of Biological Science & Engineering, Fuzhou University, Fuzhou, China
[3] Nihon Inemoto Co., LTD, Tokyo, Japan
[4] Fujian Children's Hospital, Fuzhou, Fujian, China
[5] Skin Lane (Guang Zhou) Biotech Co., Ltd., Guangzhou, China

---

1. Introduction

Probiotics are a group of live, active microorganisms that colonize in the body and altering the composition of the flora, thus benefiting the host's health [1].These microorganisms play a key role in maintaining intestinal microecological balance. Since the 1960s, with the development of microbiology, the potential of probiotics in the prevention and treatment of disease has been explored [2] [3]. However, the survival and activity of oral probiotics are affected by the harsh environment in gastrointestinal environment [4], and competition for adhesion sites with the intestinal flora remains a key challenge [5,6].Probiotic resistance to the gastrointestinal environment *in vivo* can be improved by designing effective encapsulation systems. Several bulk encapsulation systems have been used to encapsulate and protect probiotics, including emulsions[7], powder particles[8], gels[9], electrospray capsules[10], and nanofibers[10]. But the inability to control probiotic leakage[11] and particle size[12], as well as low in vivo efficacy, limit the clinical effectiveness of these batch encapsulation techniques. In response to the challenges faced by bulk encapsulation, single-cell encapsulation of individual probiotic cells with nanocoating has emerged as a viable option. Probiotic single-cell encapsulation methods include layer-by-layer assembly, phospholipid film hydration, and biofilm methods [13]. All of the above methods have the problems of cumbersome preparation, long cycle time, and difficult to scale-up production. To this end, the present work aims to apply the flash nanoprecipitation (FNP) technology in nanoparticle preparation to probiotic nanoencapsulation, and to develop efficient and high-throughput probiotic nanoencapsulation technology.

In recent years, Johnson and Prud'homme[14] proposed the FNP method, in which hydrophobic molecules and surfactants are dissolved in an organic solvent, and are turbulently mixed with an antisolvent via a mixer with confined mixing chamber to promote the

formation of nanoparticles [15]. The FNP is superior to microfluidics technology, with control of the nanoparticle size, dispersibility and reproducibility, and high yield, easiness to scale up and industrialization. Liu et al[16,17] further developed a multi-channel vortex mixer (MIVM) with four inlets [18], which allows more efficient mixing of multiple solvents in an unlimited order. Such FNP method and MIVM has been widely used for a variety of nanoparticle preparations. Since the nanoencapsulation of probiotics is in principle based on the precipitation and depositional growth of wrapping materials on the bacterial surface, which is similar to the nucleation and growth of nanoparticles, we propose that the rapid deposition and wrapping of encapsulating materials on the bacterial surface can also be achieved using the FNP technique to realize single-cell nanoencapsulation of probiotics. In this study, we attempted to apply flash nanoprecipitation (FNP) technology in conjunction with polyelectrolyte complexes (PEC) and lipid layers/liposomes (Lipo) for the nano-encapsulation of probiotics. We name this technique as Flash Nanoencapsulation (FNE). The aim is to provide gastrointestinal environment resistance and intestinal adhesion for probiotics while achieving easy, rapid and scalable production.

2. Materials and Methods

2.1. Materials

The following chemicals and biologicals were used in this study: PolyLysine (Plys, Aladdin, AR), Methacrylic Acid and Ethyl Acrylate Copolymer (L100, Aladdin, AR), Sodium polystyrene sulfonate (PSS, Aladdin, AR), lecithin (Aladdin, ≥98%), cholesterol (Sigma,≥92.5%), Fluorescein isothiocyanate (FITC, Aladdin, 95%), Rhodamine B (Aladdin), DSPE-FITC (RuiXiBIO,95%), Did (Aladdin), Hoechst 33342 (Aladdin,≥98%), MRS broth medium (Guangdong Huankai Microbial Sci. & Tech. Co., Ltd.), MRS agar medium (Guangdong Huankai Microbial Sci. & Tech. Co., Ltd.), pepsin (Solarbio), trypsin (Sinopharm Chemical Reagent Co., Ltd.), bile salt (Solarbio,BR), mucin (Yuanye Bio), PBS (MeilunBio,cell culture grade), NaCl (Sinopharm Chemical Reagent Co., Ltd), $CaCl_2$ (Aladdin, GR), NaOH (Sinopharm Chemical Reagent Co., Ltd), HCl (Sinopharm Chemical Reagent Co., Ltd).

2.2. Strain and culture conditions

The probiotic of Lacticaseibacillus rhamnosus GG (LGG) was obtained from ATCC 53103. The probiotic of P.pentosaceus (P.p) was obtained from Fuzhou University Strain Library. Probiotics were added to MRS liquid medium at 0.2% v/v and incubated in a thermostatic incubator at 37°C for 24 h for probiotics culture suspension preparation.

2.3. Encapsulation of LGG with Plys and L100

As shown in Figure 1a, Plys solution（2.0 g/L, pH 5.6）was thoroughly mixed with an equal volume of LGG culture suspension at a 1:1 volume ratio (labeled as LGG@Plys). The LGG@Plys solution was injected into the mixing chamber through ports A and B (flow rate of 18.75 mL/min), while the L100 solution (4.0 g/L, pH 8.0) was injected into the mixing chamber through ports C and D (flow rate of 15.38 mL/min) at a LGG@Plys:L100 volume ratio of 0.8. Finally, the polyelectrolyte-coated LGG solution (LGG@Plys L100) was rapidly formed in the mixing chamber.

2.4. Encapsulation of LGG@Plys L100 with liposome

Accurately weighed 1.50 g of lecithin and 0.56 g of cholesterol were added to 10 mL of anhydrous ethanol to form an ethanol solution of liposome feedstock. As shown in Figure 1b, The polyelectrolyte-encapsulated LGG solution (LGG@Plys L100) was passed into ports A, B,

and C (the flow rate of A and C was 37.50 mL/min), and the lecithin-cholesterol ethanol solution was passed into port D (the flow rate of B and D was 4.55 mL/min), so that they could rapidly form polyelectrolyte and liposome-encapsulated LGG solutions in the mixing chamber of the multichannel mixer (LGG@Plys L100@Lipo).

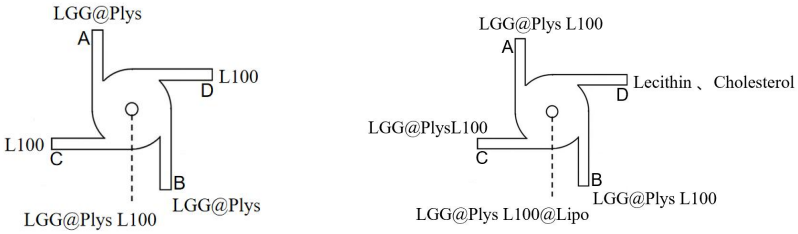

(a) (b)

Figure 1. Schematic diagram of FNP technology encapsulating LGG. (a) LGG@Plys L100. (b) LGG@Plys L100@Lipo

2.5. Encapsulation of P.p with Plys and PSS

Plys solution (2 g/L, pH 5.6) was thoroughly mixed with an equal volume of P.p culture medium bacterial precipitate in a 2:1 ratio (labeled as P.p@Plys). The P.p@Plys solution was injected into the mixing chamber through ports A and C (flow rate of 37.50 mL/min), while the PSS solution (4g/L, pH 5.6) was injected into the mixing chamber through ports B and D (flow rate of 15.28 mL/min) at a ratio of LGG@Plys: L100 volumetrically of 2.4. Finally, the polyelectrolyte-coated P.p solution (P.p@Plys PSS) was rapidly formed in the mixing chamber.

2.6. Encapsulation of P.p@Plys PSS with liposome

This step is the same as the preparation process of LGG@Plys L100@Lipo.

2.7. Characterization of LGG@Plys L100 and LGG@Plys L100@Lipo

The morphologies of LGG@Plys L100 and LGG@Plys L100@Lipo were visualized by transmission electron microscopy (TEM). Briefly, one drop of cleaned bacterial solution was placed and air-dried on the carbon-coated copper grid for TEM imaging. The encapsulation of LGG@Plys L100 and LGG@Plys L100@Lipo were also characterized by laser scanning confocal microscopy (LSCM). Briefly, 1.0 mL of 0.5 mg/mL of Hoechst 33342 was added to LGG sample to stain the cells. Hoechst 33342-labeled LGG was then encapsulated with rhodamine B-labeled polylysine and FITC-labeled L100 using previous steps and fluorescently imaged by LSCM. The lipid encapsulation was carried out (L100 was not fluorescently labeled in this process) and fluorescence imaging was also performed by LSCM.

2.8. In vitro simulation of gastrointestinal resistance

Equal LGG, LGG@Plys L100 and LGG@Plys L100@Lipo were separately subjected to simulate gastric fluid (SGF, pH 2.0) supplemented with pepsin (0.32%, w/v), simulated intestinal fluid (SIF, pH 6.8) supplemented with trypsin (0.3% w/v) and bile salt (pH 6.8), and incubated at a shaking speed of 220 rpm at 37°C. At predetermined time points, the samples were washed and coated on MRS agar plates. The colonies were counted after 24 h of incubation at 37°C.

2.9. In vitro simulation of intestinal adhesion

In vitro gastrointestinal adhesion simulations were performed using Quartz Crystal Microbalance with Dissipation Monitoring (QCM-D). After loading the gold chip and determining all frequencies, PBS buffer was passed to establish a baseline, and the following solutions were passed in sequence: 0.5 mg/mL mucin solution, phosphate buffer, sample, phosphate buffer. At the end of the experiment, the frequency/dissipation changes of the 3rd-13th octave harmonics were recorded and the adsorption data were analyzed using Qsense Dfind software.

3. Results

3.1. Characterization of LGG@Plys L100 and LGG@Plys L100@Lipo

We first investigated the encapsulation status of the probiotics. Compared to the smooth surface of LGG and P.p, the encapsulated LGG and P.p showed clear coatings on their surfaces, which confirmed the nanoscale encapsulation of the probiotics (Fig. 2). The polyelectrolyte encapsulated LGG and P.p presented a wrapping shell of couple hundred nanometers, while the polyelectrolyte/lipid double encapsulated samples showed a thicker shell. Minor aggregates were also observed on the double encapsulated LGG, likely due to the lipid aggregation. From the LSCM image, we can also see that the fluorescence of both probiotics and encapsulating materials have colocalizated, further confirming the successful encapsulation (Fig. 3).

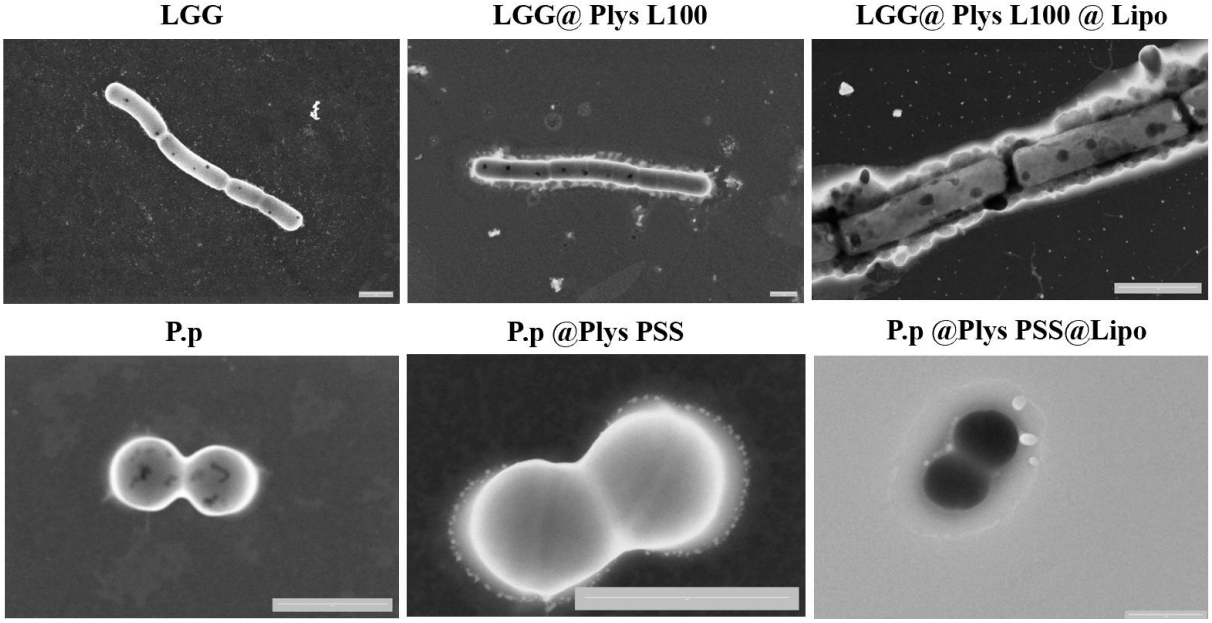

Figure 2. Transmission Electron Microscope Image of (A) LGG systems; (B) P.p systems (scale:1 μm)

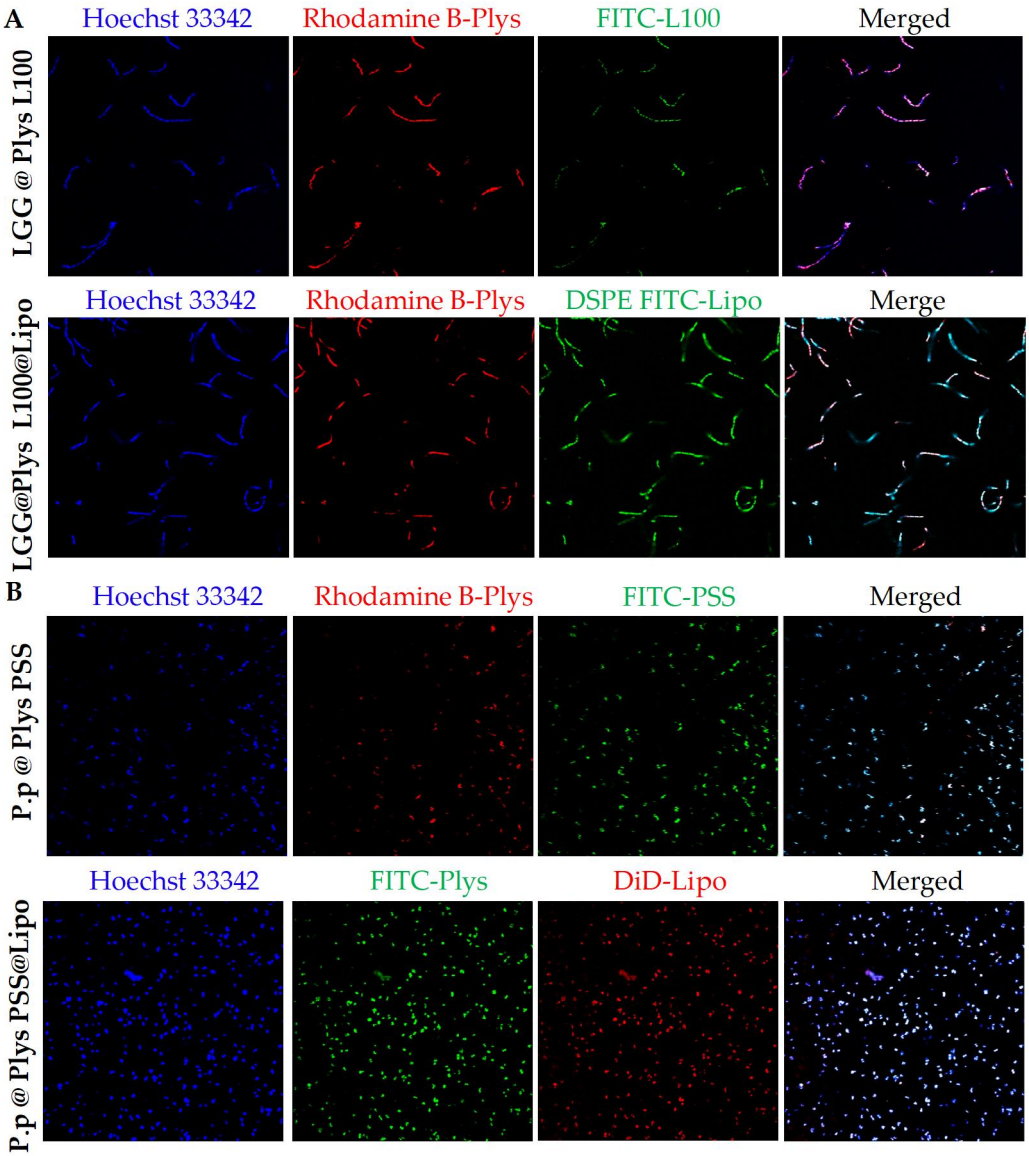

Figure 3. Laser Scanning Confocal Microscope Image of LGG and Encapsulation System (A) LGG; (B) P.p

3.2. In vitro simulation of gastrointestinal resistance

To demonstrate the probiotics-protecting ability of nanoencapsulation against the harsh gastrointestinal environment, we further tested the resistance of encapsulated probiotic against simulated gastric intestinal fluids (Fig. 4). We can see that, in all tested environments, the survival rates of probiotics after encapsulation is significantly higher than that of free probiotics, indicating that encapsulation significantly enhances the resistance of probiotics to gastric juice, intestinal fluid, and bile salts. The polyelectrolyte-lipid double encapsulated LGG and P.p showed that highest survival rates (several orders of magnitudes higher than those of naked probiotics).

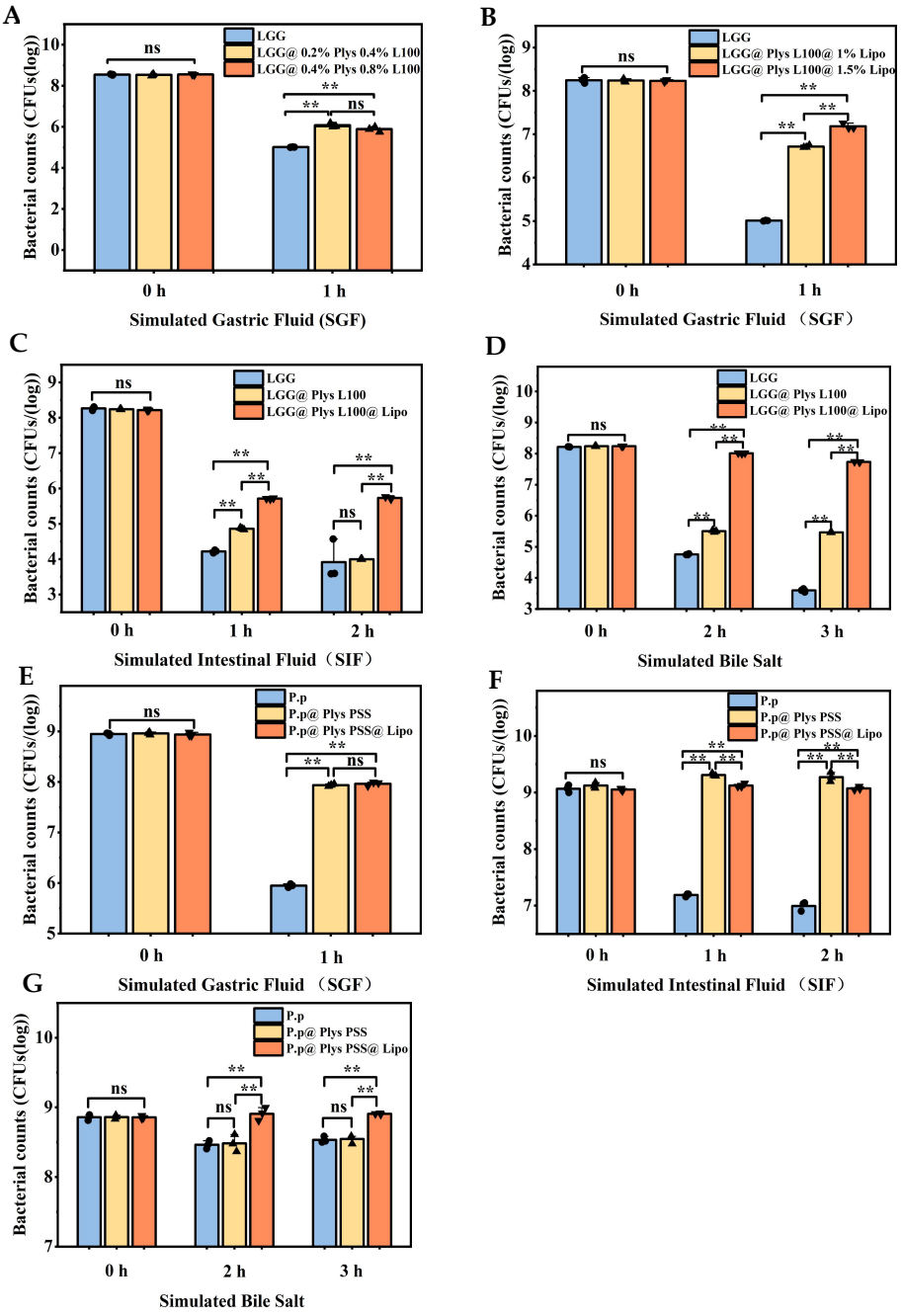

Figure 4. Resistance of gastric juice, intestinal fluid, and bile salt in LGG and P.p encapsulation systems (A-D) LGG system; (E-G) P.p system

3.3. In vitro simulation of intestinal adhesion

To simulate the colonization ability of encapsulated probiotics, we further used QCMD to test their adhesion on mucin layer. The naked bacteria showed little adhesion with minimal frequency shift (Fig. 5A, 5F, 5G). Both of the polyelectrolyte complexes and lipids showed significant adhesion on mucin layer (Fig. 5B, 5C), which promoted the adhesion of encapsulated probiotics (Fig. 5D, 5E, 5H, and 5I).

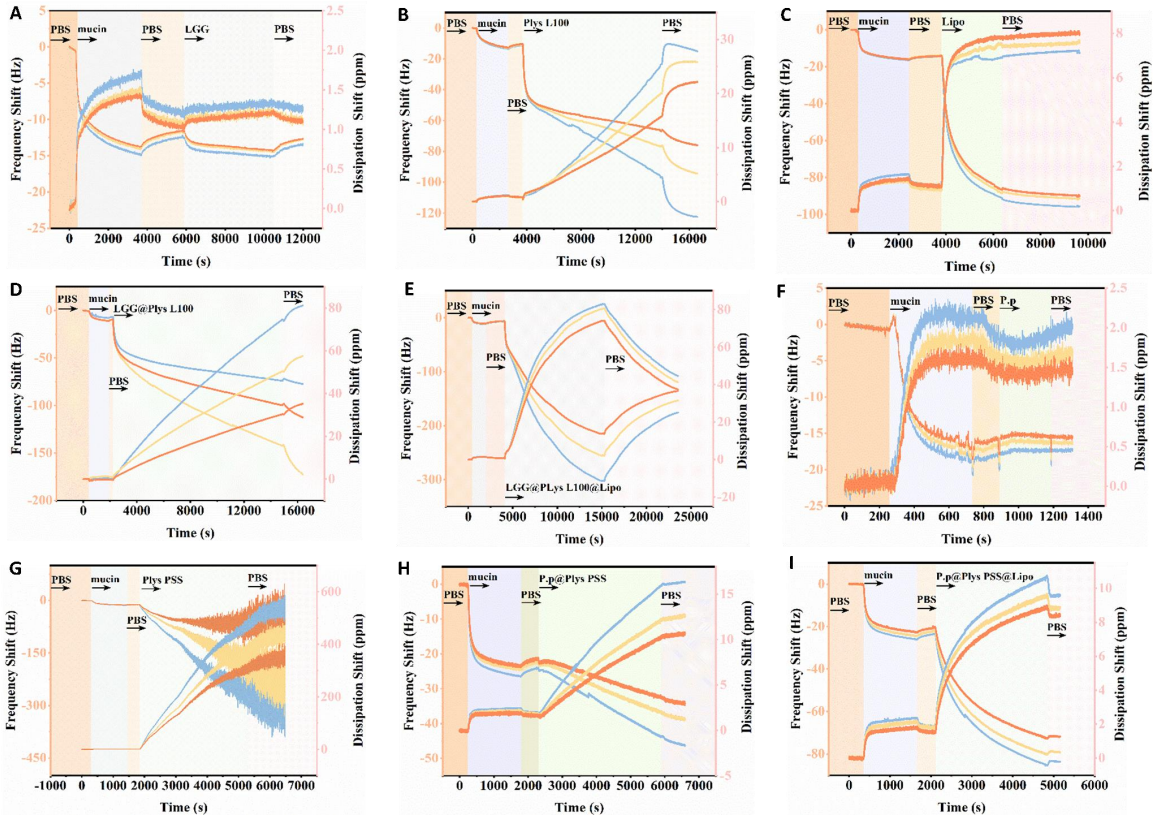

Figure 5. Frequency and dissipation shift upon adhesion of different components onto mucin coated gold chip (A) LGG; (B) Plys L100; (C) Lipo; (D) LGG@Plys L100; (E) LGG@Plys L100@Lipo; (F) P.p; (G) Plys PSS; (H) P.p@Plys PSS; (I) P.p@Plys PSS@Lipo

4. Discussion

4.1. Preparation and characterization of encapsulated probiotics

Comparing to the traditional “batch mixing” and “membrane hydration” method of nanoencapsulation, which produce encapsulated probiotics in a batch to batch mode with yield largely determined by the batch volume and processing time (normally over 10s of hours a batch), the FNE method could achieve continuous production at 60 mL/min with a single bentchtop mixer. The encapsulation status was also homogeneous as determined by both TEM and LSCM as shown in figure 2 and 3.

4.2. In vitro resistance of encapsulated probiotics against GI tract environment

The gastrointestinal resistance of probiotics is particularly important to its ability to colonize the intestinal tract. As shown in Fig. 4A, after 1 h of SGF incubation, the survival rate of free LGG decreased significantly from 108 to 105 CFU/mL, while the survival rate of PEC encapsulated LGG was one order of magnitude higher(106 CFU/mL), mainly due to the fact that the L100 is insoluble in the gastric acid environment, thus effectively blocking the attack of gastric juice on LGG. In further study, 2.0 g/L Plys and 4.0 g/L L100 were chosen as the concentrations of polyelectrolytes, based on which a second layer of liposome encapsulation was constructed. As shown in Fig. 4B, after 1 h of SGF, the PEC-lipid double encapsulated LGG survival rate reached 107 CFU/mL. This ultra-high survival rate is because lipid encapsulation covered the bacteria with a hydrophobic shell, avoiding direct contact of LGG with acids and digestive enzymes. The survival rate of free P.p and P.p after single and

double-layer encapsulation showed similar trends in SGF (Fig. 4E). in simulated intestinal fluid, In intestinal fluid, as shown in Fig. 4C, after two hours of incubation, the survival of free LGG, monolayer and bilayer encapsulated LGG, was 3.83×104, 9.95×104, and 5.4×105 CFU/mL, respectively. Meanwhile the survival of free P.p, monolayer encapsulated, and double layer encapsulated P.p was 1×107, 7.7×108 and 1.2×109 CFU/mL, respectively (Fig. 4F). Both bacteria showed significant protection from PEC-lipid double layer encapsulation, which improved the survival rate by over two orders of magnitudes. Moreover, as shown in Fig. 4D and G, the survival of LGG and P.p after encapsulation was also much higher than that of free probiotic bacteria after 2h and 3h of bile salt simulation. In summary, the nanoencapsulation of polyelectrolytes as well as lipids significantly enhanced the gastrointestinal resistance of probiotics.

4.3. In vitro simulation of intestinal adhesion by QCM-D

The adherence ability of probiotics in the intestinal tract is crucial to their probiotic effects. Probiotics form a protective layer by adhering closely to the intestinal mucosal epithelial cells, effectively preventing the intestinal tract from pathogenic bacteria. Moreover, the adherence ability of probiotics helps them to colonize and proliferate in the intestinal tract, thus maintaining the micro-ecological balance. Thus, the adhering ability of encapsulated probiotics need to be carefully investigated.

As shown in Fig. 5A, after LGG was introduced into the mucin layer, its adsorption frequency only slightly increased from 12.50 Hz to 13.30 Hz, indicating that the adhesion of LGG on the mucin surface is relatively weak. The adsorption frequency of the encapsulating material Ply@L100 rapidly rose from 10.80 Hz to 97.60 Hz, strongly demonstrating that Ply@L100 has a significantly higher adhesion than LGG (Fig. 5B). Similarly, the adsorption frequency of liposomes (Lipo) jumped from 14.0 Hz to 92.40 Hz, showing a strong adhesion of lipid on mucin layer (Fig. 5C). After encapsulated by PEC single layer and PEC-Lipid double layers, the encapsulated LGG showed the final adsorption frequencies reaching 123.94 Hz and 180.29 Hz, respectively (Fig 5D, 5E). This demonstrated the strong enhancement of PEC and lipid encapsulation on the mucin adhesion ability of LGG. Similar results was also observed with P.p, where the naked P.p showed little adhesion on mucin (Fig. 5F), while the PEC and PEC-lipid encapsulated P.p was much stronger and faster (Fig. 5H, 5I). In summary, the encapsulation materials (PEC and lipid) have significant advantages in enhancing the intestinal colonization ability of probiotics, which provides solid support for the effective colonization of probiotics in the intestine and their physiological functions.

5. Conclusion

In summary, we successfully utilized FNP technology, combined with polyelectrolytes and lipids, to encapsulate LGG and P.p, demonstrating the potential of FNP technology in bacterial nanoencapsulation. At the same time, in vitro resistance experiments showed that polyelectrolyte and lipid bilayer nanoencapsulation provided excellent gastrointestinal resistance for probiotics. In addition, we applied the dissipative quartz crystal microbalance technology (QCM-D) to simulate intestinal adhesion experiments. The results showed that the adsorption ability of free probiotics on the surface of mucin was poor, while the adhesion ability was significantly improved after single-layer encapsulation with polyelectrolytes and double-layer encapsulation with polyelectrolytes combined with lipids, providing a solid support for their probiotic effects in vivo.

References

[1] Hill C, Guarner F, Reid G, et al. The International Scientific Association for Probiotics and Prebiotics consensus statement on the scope and appropriate use of the term probiotic[J]. Nature Reviews Gastroenterology & Hepatology, 2014, 11(8): 506-514.

[2] Lim E S, Wang D, Holtz L R. The Bacterial Microbiome and Virome Milestones of Infant Development[J]. Trends in Microbiology, 2016, 24(10): 801-810.

[3] Wan M L Y, Ling K H, El-Nezami H, et al. Influence of functional food components on gut health[J]. Critical Reviews in Food Science and Nutrition, 2019, 59(12): 1927-1936.

[4] Sarao L K, Arora M. Probiotics, prebiotics, and microencapsulation: A review[J]. Critical Reviews in Food Science and Nutrition, 2017, 57(2): 344-371.

[5] Wang C, Nagata S, Asahara T, et al. Intestinal Microbiota Profiles of Healthy Pre-School and School-Age Children and Effects of Probiotic Supplementation[J]. Annals of Nutrition and Metabolism, 2015, 67(4): 257-266.

[6] Sierra S, Lara-Villoslada F, Sempere L, et al. Intestinal and immunological effects of daily oral administration of Lactobacillus salivarius CECT5713 to healthy adults[J]. Anaerobe, 2010, 16(3): 195-200.

[7] Frakolaki G, Giannou V, Kekos D, et al. A review of the microencapsulation techniques for the incorporation of probiotic bacteria in functional foods[J]. Critical Reviews in Food Science and Nutrition, 2021, 61(9): 1515-1536.

[8] Gharsallaoui A, Roudaut G, Chambin O, et al. Applications of spray-drying in microencapsulation of food ingredients: An overview[J]. Food Research International, 2007, 40(9): 1107-1121.

[9] Zhang Y, Lin J, Zhong Q. The increased viability of probiotic Lactobacillus salivarius NRRL B-30514 encapsulated in emulsions with multiple lipid-protein-pectin layers[J]. Food Research International, 2015, 71: 9-15.

[10] Rostamabadi H, Assadpour E, Tabarestani H S, et al. Electrospinning approach for nanoencapsulation of bioactive compounds; recent advances and innovations[J]. Trends in Food Science & Technology, 2020, 100: 190-209.

[11] Trush E A, Poluektova E A, Beniashvilli A G, et al. The Evolution of Human Probiotics: Challenges and Prospects[J]. Probiotics and Antimicrobial Proteins, 2020, 12(4): 1291-1299.

[12] Asgari S, Pourjavadi A, Licht T R, et al. Polymeric carriers for enhanced delivery of probiotics[J]. Advanced Drug Delivery Reviews, 2020, 161: 1-21.

[13] Xu C, Ban Q, Wang W, et al. Novel nano-encapsulated probiotic agents: Encapsulate materials, delivery, and encapsulation systems[J]. Journal of Controlled Release, 2022, 349: 184-205.

[14] Johnson B K, Prud'homme R K. Flash NanoPrecipitation of organic actives and block copolymers using a confined impinging jets mixer[J]. Australian Journal of Chemistry, 2003, 56(10): 1021-1024.

[15] Morozova T I, Lee V E, Panagiotopoulos A Z, et al. On the Stability of Polymeric Nanoparticles Fabricated through Rapid Solvent Mixing[J]. Langmuir, 2019, 35(3): 709-717.

[16] Liu Y, Cheng C Y, Liu Y, et al. Mixing in a multi-inlet vortex mixer (MIVM) for flash nano-precipitation[J]. Chemical Engineering Science, 2008, 63(11): 2829-2842.

[17] Russ B, Liu Y, Prud'homme R K. OPTIMIZED DESCRIPTIVE MODEL FOR MICROMIXING IN A VORTEX MIXER[J]. Chemical Engineering Communications, 2010, 197(8): 1068-1075.

[18] Liu Y, Cheng C, Liu Y, et al. Mixing in a multi-inlet vortex mixer (MIVM) for flash nano-precipitation[J]. Chemical Engineering Science, 2008, 63(11): 2829-2842.